# Investigating strain-induced crystallization through fatigue striations in filled NR

Benoît Ruellan, Jean-Benoit Le Cam, Eric Robin, I. Jeanneau, F. Canévet, G. Mauvoisin, D. Loison

# Investigating strain-induced crystallization through fatigue striations in filled NR

B. Ruellan*†‡, J.-B. Le Cam*†, E. Robin*†, I. Jeanneau‡†, F. Canévet‡†, G. Mauvoisin & D. Loison*

* *Univ Rennes, CNRS, IPR (Institut de Physique de Rennes), UMR 6251, Rennes, France*

*† LC-DRIME, Joint Research Laboratory, Cooper Standard - IPR, UMR 6251, Rennes Cedex, France*

*‡ Cooper Standard France, Rennes, France*

* *Laboratoire de Génie Civil et Génie Mécanique EA 3913, IUT-Université de Rennes 1, France*

ABSTRACT: Natural Rubber (NR) exhibits a remarkable fatigue resistance, especially for non-relaxing loadings under which a strong lifetime reinforcement is observed (Cadwell et al. 1940). Such a resistance is classically attributed to strain-induced crystallization (SIC). At the microscopic scale, it has been shown that SIC induces striations on the fracture surface of NR samples tested under fatigue loadings (Le Cam and Toussaint 2010, Muñoz-Mejia 2011, Le Cam et al. 2013, Ruellan et al. 2018). In order to provide additional information on the role of SIC in the fatigue crack growth resistance of NR, striations are investigated through post-mortem analysis after fatigue experiments carried out under both relaxing and non-relaxing loadings. Results show that two striation regimes take place. Regime 1 corresponds to small striation patches with different orientations and Regime 2 induces zones with large and well-formed striations. As fatigue striations are observed for all the loading ratios applied, they are therefore not the signature of the reinforcement. Nevertheless, increasing the minimum value of the strain amplified the striation phenomenon and the occurrence of Regime 2. The analysis carried out unifies the results obtained in the literature for relaxing and fully relaxing loadings in the sense that increasing the loading, *i.e.* the tearing energy, leads to an increase in the crack growth rate Lindley (1973) and to a striation typology evolution, especially the striation size (Ruellan et al. 2018).

## 1 INTRODUCTION

Elastomeric materials exhibit strong damping abilities as well as a high fatigue resistance. Thanks to these extraordinary mechanical properties, they are used in many applications. The fatigue properties of NR were investigated as soon as the 1940s by the pioneer work by (Cadwell et al. 1940), Fielding (1943) and many years later by Beatty (1964). Typically, it was shown that the fatigue life of NR improves when it is tested under non-relaxing loadings (*i.e.* $R^1 > 0$). Since this was not observed in the case of non-crystallizable rubbers, this outstanding property was attributed to SIC. Under an increasing loading ratio R and considering the crack growth approach, this effect leads to a decrease of the crack growth rate and the tearing energy below which no crack growth occurs (Lindley 1973), under non-relaxing loadings. In the following, the term "lifetime reinforcement" will denote both the improvement of the fatigue life (*i.e.* considering the crack initiation approach) and the crack propagation delay (*i.e.* considering the crack propagation approach) observed under non-relaxing loadings. Even though this phenomenon has been observed for decades, the mechanisms of crack growth in NR, especially under non-relaxing conditions are not fully established, which is an obstacle for lifetime prediction. The activation of SIC can be observed on the failure surface of NR samples by the presence of certain motphological patterns, namely wrenchings and striations (le Cam et al. 2013). Therefore, it could be assumed that their formation at the fracture surface of NR samples is the signature of the crack growth reinforcement due to SIC at the microscopic scale. The formation mechanism of wrenching was established in le Cam et al. (2004). The authors showed the role of SIC on their process of formation: highly crystallized ligaments form between elliptical zones where the crack propagates, which delays the crack propagation. This is in a strong contrast with non-crystallizable rubbers, where no such ligaments form (le Cam et al. 2014). Contrarily, the formation mechanism of fatigue striation is not clearly established even though it seems to be imputed to SIC. Four studies investigated fatigue striations (Le Cam and Toussaint 2010, Flamm et al. 2011, Muñoz-Mejia 2011, Le Cam et al. 2013), only the paper by Le Cam and Toussaint (2010) was fully dedicated to

1 R is the loading ratio, defined as the ratio between the minimum and the maximum of the loading

their study. The presentation of the experimental conditions used in the above mentioned papers are detailed in Ruellan et al. (2018), they are therefore not provided here. The state of the art carried out revealed that different loading conditions were used, which led to different results in terms of striation typology and morphology. Therefore, the comparison between them has to be done with respect to the sample geometry and no generalization to NR can be done. A new study including non-relaxing loadings and elevated temperatures is therefore carried out in order to to provide new elements on the role of SIC in the crack growth resistance of NR. The experimental setup is presented in the next section, results are given and discussed, concluding remarks close the paper.

## 2 EXPERIMENTAL SETUP

### 2.1 *Material and sample geometry*

The material considered is a carbon black filled natural rubber (*cis*-1,4 polyisoprene) vulcanised with sulphur. Samples tested are Diabolo samples.

### 2.2 *Loading conditions*

The fatigue tests were performed with a uni-axial MTS Landmark equipped with a homemade experimental apparatus. This apparatus enables us to test simultaneously and independently eight Diabolo samples, which reduces the fatigue test duration.

The tests were performed under prescribed displacement. The corresponding local deformation at the sample surface in the median zone was calculated by finite element analysis (FEA). In order to investigate the effect of temperature, a Servathin heating chamber was used and three temperatures were applied: 23, 90 and 110°C. A pyrometer tracked the temperature of a material point located in the Diabolo median surface. For that purpose, a second homemade system has been developed to provide the suitable kinematics to the pyrometer. The frequency was chosen in such a way that the global strain rate $\dot{\varepsilon}$ was kept constant, ranging between 1.8 and 2.4 $s^{-1}$ for one test to another one, in order to limit self-heating. In practice, the frequency ranged between 1 and 4 Hz, depending on the strain amplitude. Five different loading ratios $R_\varepsilon = \frac{\varepsilon_{min}}{\varepsilon_{max}}$ were used: -0.25; 0; 0.125; 0.25 and 0.35. One recall that loading ratios inferior, equal and superior to zero correspond to tension-compression, repeated tension and tension-tension loadings, respectively.

### 2.3 *Scanning Electron Microscopy*

Second electrons images of Diabolo fracture surfaces are stored with a JSM JEOL 7100 F scanning electron microscope (SEM). In addition, the SEM is coupled with an Oxford Instrument X Max energy dispersive spectrometer of X-rays (EDS) and an Aztzec software in order to determine the surface fracture composition, especially in the crack initiation zone. The fracture surfaces to be analysed are previously metallized by vapour deposition of an Au-Pd layer.

## 3 RESULTS

The spatial distribution of fatigue striations is described, then the effects of the loading on their occurrence and on their typology are presented.

### 3.1 *Spatial distribution of the fatigue striations*

Both optical microscopy and SEM were used to investigate fatigue striation at the microscopic scale. Figure 3 shows a typical Diabolo fracture surface after a fatigue test carried out at $R_\varepsilon = 0$, $\varepsilon_{max} = 150\%$ and at a frequency of f = 1.5 Hz.

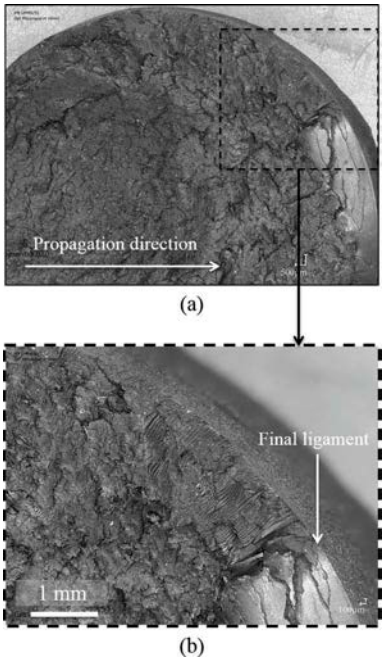


Figure 1. spatial distribution of fatigue striations: (a) Diabolo fracture surface and (b) zoom on the striation zone, close to the final ligament.

The spatial distribution of the fatigue striations is generally in good agreement with literature (Le Cam and Toussaint 2010, Le Cam et al. 2013) since they precede the final ligament in the crack propagation process. At this stage, the stress level has increased in comparison to the beginning of the crack propagation, since the tests are prescribed under displacement. Note that fatigue striations mainly appeared along the edge of the sample. They peopled the bulk when the

loading applied increased. Finally, an increase in the striation number is observed as the surface gets closer to the final ligament.

### 3.2 *Typology of the fatigue striations*

Two fatigue striation typologies are observed and represented in Figure 2. They are hereafter referred to as Regime 1 and Regime 2, respectively:

- Regime 1 stands for striation patches (see the left-hand side of Fig. 2(a)). Their orientation differs from one patch to another and wrenchings can be observed in between patches. Regime 1 striations are rather small, they are separated by a distance in the order of magnitude of 20 $\mu$m, therefore, the loading is moderate. Regime 1 seems to be a transition zone between full wrenchings and full striations zones.
- Regime 2 refers to well defined striations (see Fig. 2(b)), wrenchings are no longer observed. The surface of the striations is rather smooth and the distance separating one striation to another is larger than for Regime 1, in the order of magnitude of 100 $\mu$m. As for Regime 1, Regime 2 striations present a triangular shape. They are observed close to the final ligament, therefore, it can be considered that they form under severe loadings. Regime 2 striations were already identified in Le Cam and Toussaint (2010), Flamm et al. (2011) and Le Cam et al. (2013). Finally, it is to note that Regime 2 is always preceded by Regime 1.

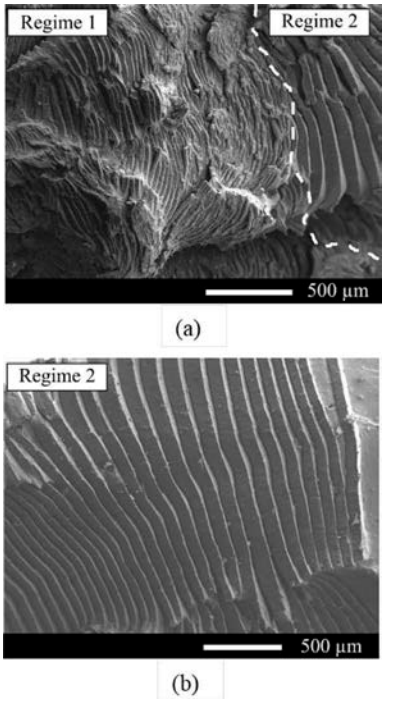


Figure 2. SEM images of the two striation regimes: (a) Regime 1 (b) Regime 2.

### 3.3 *Link between fatigue striation and loading condition*

As discussed in the introduction, NR exhibits a lifetime reinforcement due to SIC under non-relaxing loadings (*i.e.* R > 0). This phenomenon can be illustrated in a Haigh diagram and (André 1999, Saintier 2000) since it distinguishes relaxing from non-relaxing loadings. Fatigue striations are linked to the loading condition in the Haigh diagram presented in Figure 3 in order to bring new information on the role of SIC in the crack growth resistance of NR. The Haigh diagram is plotted in terms of strain for fatigue tests performed at 23°C, the change of slope of the iso-lifetime curves in the non-relaxing zone highlights the classical lifetime reinforcement. More details are given in ruellan18b.

At the macroscopic scale, three damage modes are identified:

- crack initiation in the surface vicinity and propagation in the median section until the total sample failure. It is observed in the case of relaxing loadings, where no reinforcement occurs,
- crack initiation in the surface vicinity and propagation by bifurcation in the median section zone,
- crack initiation and growth below the metallic insert.

The last two damage mechanisms are observed under non-relaxing loadings, where the lifetime reinforcement takes place. This indicates that damage is strongly impacted by the loading condition and hence by SIC. Damage analysis at the microscopic scale was performed using SEM. Three fracture surface types are identified and described as follows:

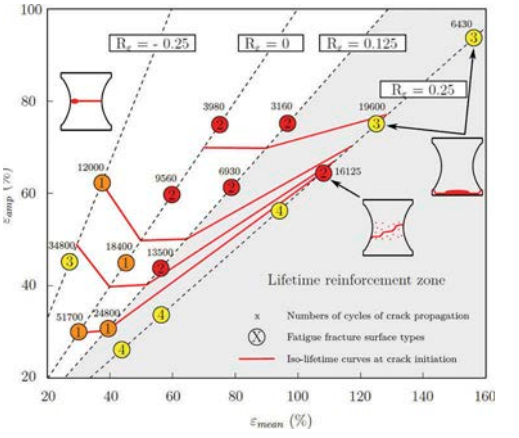


Figure 3. Haigh Diagram at 23°C.

① fracture surface exhibiting Regime 1 fatigue striations,
② fracture surface exhibiting Regime 2 fatigue striations. Since Regime 2 always follows Regime 1, it is to note that fracture surfaces denoted ② also contain Regime 1,
③ fracture surface with no fatigue striation.

Fracture surfaces ④ correspond to fatigue experiments where no crack initiation was observed after 1.5 M cycles. To go further on the effect of the loading on the fatigue striation phenomenon, the fracture surfaces are described with respect to the loading ratio $R_\varepsilon$.

#### 3.3.1 $R_\varepsilon = 0$

For repeated tension, fatigue striations are observed under all the maximal strain range applied. Regime 1 striations form under each maximal strain tested, however, Regime 2 striations only occur under a high $\varepsilon_{max}$. It is to note that both striation height and pitch increase with $\varepsilon_{max}$, which is in good agreement with Muñoz-Mejia (2011).

#### 3.3.2 $R_\varepsilon > 0$

For non-relaxing tension, the same comments as for repeated tension can be drawn. However, Regime 2 is observed under less important $\varepsilon_{max}$. Therefore, it is concluded that $\varepsilon_{min}$ also influences the fatigue striation phenomenon. As pointed out by Borgarino et al. (2013), the crystallinity never goes back to zero during a non-relaxing fatigue experiment. It could indeed promote the occurrence of Regime 2. Note that no striation is observed for the two most severe loadings at $R_\varepsilon = 0.25$. It can be explained by the fact that the damage mechanisms differed from the one at lower $\varepsilon_{max}$: the crack initiated and propagated in a region below the metallic insert were a high hydrostatic pressure occurs.

#### 3.3.3 $R_\varepsilon < 0$

For tension-compression, Regime 1 striations form under higher $\varepsilon_{max}$ than for repeated tension and Regime 2 did not occur in the loading range investigated. This result can be explained by the fact that the crystallinity is expected to go back to zero between each cycle of such a fatigue experiment.

#### 3.3.4 *Effect of the temperature*

The previous results highlighted the strong influence of the loading on the occurrence of fatigue striation. Typically, the striation formation seems to be encouraged under $R_\varepsilon > 0$ loadings, where the lifetime reinforcement due to SIC occurs. To confirm the role of SIC in the striation formation process, fatigue experiments performed at 23°C were also carried out at 90°C where the crystallinity under quasi static loading is zero or very close to zero (Trabelsi et al. 2002) and the fatigue life reinforcement less pronounced (Ruellan et al. 2018). No striation is observed, therefore, it is concluded that a certain amount of crystallinity is required for striations to form.

## 4 DISCUSSION

At 23°C, striations form whatever the loading applied (*i.e.* even under $R_\varepsilon < 0$ loadings, where no lifetime reinforcement occurs). It indicates that striations are not the signature of the lifetime reinforcement due to SIC.

At 90°C where the crystallinity is very low, no striation form even under large $\varepsilon_{max}$. Therefore, it is concluded that striations are the signature of SIC and that a certain amount of crystallinity is required for them to form.

Our results put into light the formation of two types of fatigue striations: Regime 1 composed of striation patches and observed under a wide range of loadings including relaxing ones and Regime 2 corresponding to well defined striations and is only observed under non-relaxing loadings. Furthermore, the striation formation is amplified under non-relaxing loadings. These results are put into perspective with the study by Lindley (1973) from which two main results can be deduced: *(i)* increasing the tearing energy (*i.e.* the loading) facilitates the propagation. In other words, the more important the loading, the more encouraged the crack propagation, *(ii)* for a given tearing energy, increasing the loading ratio decreases the crack growth rate. This result highlights the fact that the crack propagation is delayed under non-relaxing loadings, due to SIC. This is typically what was observed under $R_\varepsilon = 0.25$ loadings. Firstly, no failure occurred below $\varepsilon_{max} = 65$ % which is consistent with the delay in crack propagation (see fracture surface ④). Under superior $\varepsilon_{max}$, only Regime 2 occurred. Secondly, according to Lindley's results, the crack growth rate at which Regime 2 occurs under $R_\varepsilon = 0.25$ loadings should be lower than the one at which it occurs under lower loading ratios. To verify this result, the number of cycles of crack propagation denoted $N_p$ is calculated, it corresponds to the number of cycles between crack initiation and total failure. As the fatigue tests were performed under a quasi-constant strain rate, it can be concluded that the crack growth rate evolves with the invert of $N_p$. Note that the $N_p$ values are reported in Fig. 3. For a given strain amplitude, since $N_p$ increases with the loading ratio, the crack growth rate decreases which confirms Lindley's results. It also suggests that the striation typology is driven by the crack growth rate.

## 5 CONCLUSION

The present study investigates the crack growth resistance of NR by post-mortem analysis of Diabolo samples tested under fatigue loadings. Fatigue striations are identified and found to form under two

regimes: Regime 1 corresponds to striation patches whereas Regime 2 stands for well defined striations. Since they are observed independently of the loading applied (including relaxing loading, where no lifetime reinforcement occurs), they are therefore not the signature of the reinforcement due to SIC. However, on the one hand, no striation form at 90°C where the crystallinity is very low. On the other hand, the striation phenomenon is encouraged at 23° C, especially under non-relaxing loadings, where the crystallinity remains positive. Therefore, it is concluded that striations are the signature of SIC and that a certain amount of crystallinity is required for them to form. Our results are in good agreement with Lindley's: under relaxing loadings (*i.e.* $R\varepsilon$ 0), the crack growth rate increases as the loading increases. Under non-relaxing loadings (*i.e.* $R\varepsilon > 0$), the striation typology is governed by the loading ratio.

## REFERENCES


André, N. (1999). *Critère local d'amorcage de fissures en fatigue dans un élastomère de type NR*. PhD thesis, Ecole Nationale Supérieure des Mines de Paris.

Beatty, J. R. (1964). Fatigue of rubber. *Rubber Chemistry and Technology* 37, 1341–1364.

Beurrot-Borgarino, S., B. Huneau, E. Verron, and P. Rublon (2013). Strain-induced crystallization of carbon black-filled natural rubber during fatigue measured by in situ synchrotron x-ray diffraction. *International Journal of fatigue* 47, 1–7.

Cadwell, S. M., R. A. Merril, C. M. Sloman, and F. L. Yost (1940) Dynamic fatigue life of rubber. *Industrial and Engineering Chemistry (reprinted in Rubber Chem. and Tech. 1940; 13:304-315) 12*, 19–23.

Fielding, J. H. (1943). Flex life and crystallisation of synthetic rubber. *Industrial and Engineering Chemistry* 35 (12), 1259–1261.

Flamm, M., J. Spreckels, T. Steinweger, and U. Weltin (2011). Effects of very high loads on fatigue life of nr elastomer materials. *International Journal of Fatigue* 33 (9), 1189–11198.

Le Cam, J.-B., B. Huneau, and E. Verron (2013). Fatigue damage in carbon black filled natural rubber under uni- and multiaxial loading conditions. *International Journal of Fatigue* 52, 82–894.

Le Cam, J.-B., B. Huneau, E. Verron, and L. Gornet (2004). Mechanism of fatigue crack growth in carbon black filled natural rubber. *Macromolecules* 37, 5011–5017.

Le Cam, J.-B. and E. Toussaint (2010). The mechanism of fatigue crack growth in rubbers under severe loading: the effect of stress-induced crystallization. *Macromolecules* 43, 4708–4714.

Le Cam, J.-B., Huneau, B., and Verron, E. (2014). Failure analysis of carbon black filled styrene butadiene rubber under fatigue loading conditions. *Plastics, Rubber and Composites*, 43(6):187–191.

Lindley, P. (1973). Relation between hysteresis and the dynamic crack growth resistance of natural rubber. *International Journal of Fracture* 9(4), 449–462.

Muñoz-Mejia, L. (2011). *Étude exprimentale des mécanismes d'endommagement par fatigue dans les élastomères renforcés*. PhD thesis, Université Claude Bernard Lyon 1.

Ruellan, B., J.-B. Le Cam, I. Jeanneau, F. Canévet, F. Mortier, and E. Robin (2018) Fatigue of natural rubber under different temperatures. *International Journal of Fatigue.* https://doi.org/10.1016/j.ijfatigue.2018.10.009.

Ruellan, B., J.-B. Le Cam, E. Robin, I. Jeanneau, F. Canévet, G. Mauvoisin, and D. Loison (2018). Fatigue crack growth in natural rubber: The role of sic investigated through post-mortem analysis of fatigue striations. *Engineering Fracture Mechanics* 201, 353–3365.

Saintier, N. (2000). *Prévisions de la durée de vie en fatigue du NR, sous chargement multiaxial*. PhD thesis, École Nationale Supérieure des Mines de Paris.

Trabelsi, S., P.-A. Albouy, and J. Rault (2002). Stress-induced crystallization around a crack tip in natural rubber. *Macromolecules* 35, 10054–10061.